Experimental investigation of water vapor condensation from hot humidified air in serpentine heat exchanger

R. Poškas [a], A. Sirvydas [a], M. Salem [a], P. Poškas [a], H. Jouhara [b,*]

[a] Nuclear Engineering Laboratory, Lithuanian Energy Institute, Breslaujos 3, LT-44403 Kaunas, Lithuania
[b] Heat Pipe and Thermal Management Research Group, College of Engineering, Design and Physical Sciences, Brunel University London, Uxbridge UB8 3PH, United Kingdom

ARTICLE INFO

ABSTRACT

Condensing economizers are used in industry and power plants for waste heat recovery. Despite widespread use, their thermal design is still not optimized due to the complexity of the condensation process especially when non-condensing gasses are prevalent. This paper presents an experimental study of water vapor condensation on the vertical tubes of a serpentine bundle in a humidified air crossflow at water vapor mass fractions of 10% and 20%. The analysis showed a clear dependence of the efficiency of the condensation process on the humidified air inlet temperature and Reynolds number, and the efficiency increases as these parameters decrease. Condensation efficiency also depends highly on flow humidity especially in the region of higher Reynolds numbers. A comparison of the average Nusselt number in the case of dry air with the experimentally determined average Nusselt number is also presented, and showed a uniform increase in the Nusselt number as the inlet temperature of the humidified air decreased.

1. Introduction

The European Union actively supports the conversion of inefficient technologies to efficient ones that help to reduce the amounts of waste heat. Lower energy costs as well as reduced waste heat help industry to save money and cut production prices, and hence remain competitive in the market [1]. Increased energy efficiency is also significant as an environmental issue because of lower amounts of pollution discharged into the environment. Lithuania's energy strategy provides objectives and key decisions concerning electricity, heating, gas, oil, renewable resources, increased energy efficiency, environmental safety, and lower greenhouse gas emissions. One of the strategic objectives is in the heating sector where the government is supporting initiatives that strive to increase energy consumption efficiency and encourage energy generation from waste.

In power plants, huge amounts of heat are removed through the chimney with the flue gas and, in industry during technological processes, with synthetic gas [2]. Various condensing heat exchangers are used for recovering this waste heat through the condensation process. Condensation is a common phase change process in which a vapor cools down and turns into a liquid. This liquid can be a film that adheres to the surface of the condenser. As it thickens, this film halts the heat transfer process. As such, it is called film-wise condensation. Alternatively, condensation can be in drops on the condenser's surface that fall from their place because of gravity when they reach a critical size; this process is called drop-wise condensation. The determinant factors that affect which mode will take the lead are the thermochemical properties of the condensate, characteristics of the condenser surface and operating conditions. The heat transfer coefficient in drop-wise condensation is much higher than in film-wise condensation because there is no film resistance to plummet heat transfer [3]. However, in reality, film-wise condensation dominates in many heat and mass transfer processes.

There have been many condensation investigations conducted with pure water vapor in crossflow over horizontal tubes and tube bundles [4-13, etc.]. Regarding the heat transfer coefficient of a single tube, the most appropriate correlations were suggested by Fujii et al. [6] and Rose [7]. Jakob in [4] proposed an equation for defining the relation between the Nusselt number and the condensate Reynolds number for an isothermal tube bundle. They also suggested an equation for defining the inundation factor, which represents the decrease in heat transfer due to inundation. Since the suggested equation was too conservative, an improvement was proposed by Kern in [5]. Experimental results presented in [9] have a good correlation with the Kern equation. In this work the authors proposed another equation for the inundation factor calculation.

---

* Corresponding author.
E-mail address: Hussam.Jouhara@brunel.ac.uk (H. Jouhara).

Nomenclature

Abbreviations	
HA	Humidified air
WVMF	Water vapor mass fraction
c_p	Specific heat, kJ/(kg· °C)
d	Outer diameter of the tube, m
G	Volumetric flow rate, m³/s
l	Length, m
m	Mass flow rate, kg/s
Nu	Nusselt number
$\overline{Nu}$	Average Nusselt number
Re	Reynolds number
$\overline{Re}$	Average Reynolds number
r	Latent heat of condensation, kJ/kg
S	Area, m²
t	Temperature, °C
Q	Heat quantity, W
q	Heat flux, W/m²

Greek symbols	
α	Heat transfer coefficient, W/(m². °C)
η	Condensation efficiency,%
λ	Thermal conductivity, W/(m· °C)
μ	Dynamic viscosity, kg/(m·s)
ρ	Density, kg/m³
Subscripts	
cd	Condensate
cw	Cooling water
f	Fluid (humidified air)
i	Local (row)
in	Inlet
ln	Logarithmic
t	Total (condensation and convection)
v	Water vapor
w	Wall

Investigations with vertical tubes and tube bundles are rather limited [14–16]. The authors of [15] analyzed a condensate film running along a vertical tube under vapor forced flow. In this publication, an equation for heat transfer calculations was presented. In a recent paper [16] water vapor condensation on three stainless steel vertical pipes was investigated experimentally. The pipes had been placed in a narrow channel (two channels with different widths were tested, i.e., 20.0 and 24.0 mm) and the vapor flowed in a crosswise direction. Cooling water was supplied according to the co-current flow scheme. The water vapor velocity at the inlet to the channel varied from 0.67 to 2.32 m·s⁻¹. The average Reynolds number for the cooling water was 22,000–25,000. Average temperatures of the cooling water at the inlet into the exchanger were 30, 40 and 50 °C. An analysis showed that the width of the channel did not have any effect on the condensation process. The heat flux in the heat exchanger increased with a decreasing inlet cooling water temperature, i.e., a decrease in the cooling water temperature of 20 °C increased the output of the heat exchanger by ~25%. When only some of the water vapor condensed in the heat exchanger, the influence of the water vapor velocity at the inlet to the heat exchanger was reduced. Also, the condensation heat transfer coefficient increased with a higher vapor mass flow rate (thus, a higher velocity). Finally, the experimental results were compared with the equation presented in [15]; however, the agreement with the data was not very good. Summarizing the literature review for pure water vapor,it can be stated that all the studies conclude that heat transfer is significantly improved with the condensation of pure water vapor in comparison with forced convection without condensation.

There are other studies more concerned about the impact of non-condensable gasses on the condensation process [17–19]. However, the water vapor mass fraction is usually high compared to the mass fraction of the non-condensable gasses [20–22].

In the cases of flue gas or synthetic gas, the amount of non-condensable gasses is high, and the amount of water vapor is small. Such a combination influences heat transfer significantly, see the studies on the heat transfer characteristics on a horizontal tube in a crossflow [17,23-26]. In [17] experiments were performed, where the air-vapor mixture was used to simulate the flue gas of a natural gas-fired boiler. The water vapor mass fraction was 3.2–12.8%. The experimental results showed that the convection-condensation heat transfer coefficient increased with the Reynolds number and vapor mass fraction and was 1~3.5 times that of the forced convection without condensation. A correlation was proposed to describe the combined convection-condensation heat transfer. In [23] condensation heat

transfer on horizontal stainless-steel tubes was investigated experimentally by using the flue gas from an industrial gas boiler. The experiments were conducted at different air ratios of the flue gas. The experimental data were compared with the correlation suggested by other researchers, and it was noticed that at low-wall-temperatures, the total heat transfer was higher than that predicted by the correlation. The same authors continued their research and in [24] they performed studies concerning the effects of tube stages and gas velocities at a water vapor mass fraction of 10%. It was noticed that the heat transfer was enhanced at the second tube stage due to the increased turbulence of the flow from the first stage. No significant decrease in condensation in the second stage due to the condensate falling from the first stage could be observed. Even at a high gas velocity (15 m/s, $Re \approx 13,000$), the condensation pattern was similar to that observed in the previous low gas velocity (3.5 m/s) experiments [23]. A vapor-gas mixture (water vapor mass fraction ~25%) was analyzed by the same authors in [25]. In this work, a correlation was proposed to predict condensation heat transfer for the region of the parameters analyzed. In [26], a relation was found between the local Nusselt number and Reynolds numbers by conducting an experiment on moist air condensing on a horizontal pipe heat exchanger. From their results, it can be noted that the local Nu number increased along with the Prandtl number at a certain Reynolds number. Hence, the condensation rate increased because the latent heat of condensation increased. The average Nu number increased as the temperature difference decreased at a higher Reynolds number. Additionally, a high relative humidity increased the rate of condensation, and thus the mass transfer coefficient was enhanced.

Even fewer condensation studies have been performed with vertical tubes in the presence of large amounts of non-condensable gas. There are few studies on the heat transfer characteristics inside the vertical tubes of a condensing shell and tube heat exchanger [27–29] and for a vertical tube and a tube bundle in a crossflow [30–33]. In [30] experimental tests were performed using a heat exchanger consisting of 96 tubes. The tests were performed while maintaining the following parameters: the initial cooling water temperature was 19.5 °C and the gas mixture (air-water vapor) temperature was 62–100 °C. The water vapor mass fraction varied from 0 to 40%. The results showed that with a small fraction of non-condensable gas in the gas mixture flow, the surface temperature of the condensate film was not uniform on the tubes and depended on the location of the tubes in the heat exchanger. An experimental analysis of water vapor condensation heat transfer in the presence of non-condensable gas in a vertical tube and tube bundles in crossflow is presented in [31]. During the investigations, the air mass
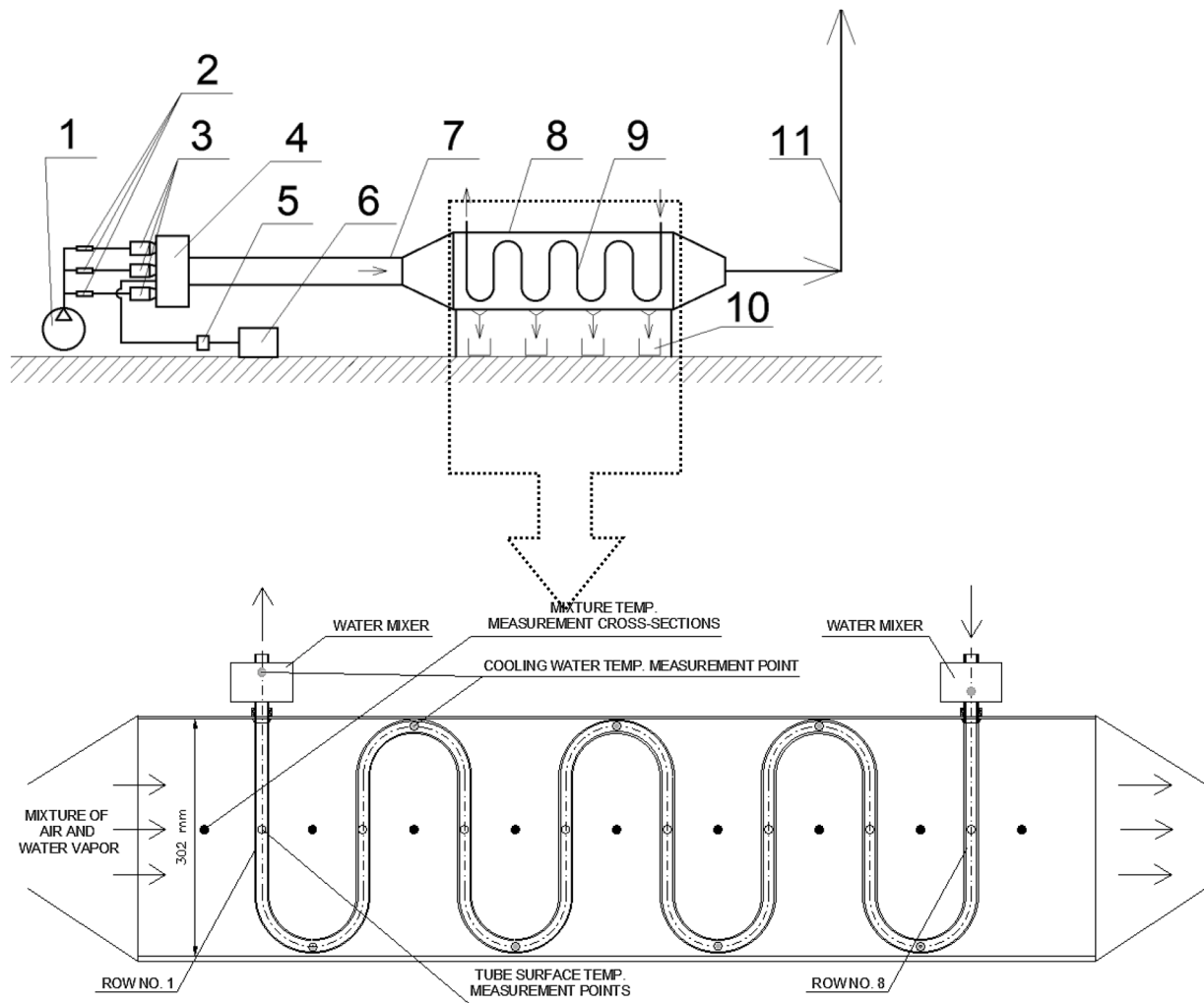
Fig. 1. Experimental setup: (1) compressor, (2) airflow rate meters, (3) air heaters, (4) air and vapor mixing chamber, (5) vapor flow rate meter, (6) steam generator, (7) 3 m long pipe, (8) test section, (9) serpentine tube bundle, (10) condensate collection bottles, (11) stack. *(2-column fittingimage.)*.

fraction was changed from 5% to 65% (water vapor mass fraction from 95% to 35%, respectively). At a low air mass fraction (5%), the average heat transfer rate of the tube bundle was approximately twice that of a single tube. As the air mass fraction increased, the heat transfer rate of the bundles decreased rapidly. In the case of a single tube, the decrease was much less pronounced. For a higher air mass fraction (from 40%), the difference between heat transfer rates in the single tube and in the tube bundle became negligible. It was also pointed out that the main factors influencing the condensation heat transfer were the thickness of the non-condensing gas layer and the water vapor flow rate. Investigations of flue gas condensation in a few heat exchangers connected in series were performed in [32], i.e., experiments were performed in three groups of connected multi-row vertical staggered tube bundle heat exchangers. The impact of multiple parameters such as the flue gas velocity, water vapor mass fraction, cooling water flow rate and cooling water temperature, on the condensation heat transfer and condensate collection rate were analyzed. The results showed that the convective heat transfer (sensible heat) was at least two times lower compared to the total (convection and condensation) heat transfer (sensible and latent heat) in each group of condensers as the flue gas velocity changed. As the flue gas velocity increased, the convective heat transfer increased linearly in all three heat exchangers, but the total heat transfer increased only up to a certain flue gas velocity and then started to decrease. Also, the differences in the total heat transfer in all three groups were quite significant, but in the case of convective heat transfer, they were

insignificant. It was noticed that the water vapor fraction was an important factor influencing the heat transfer, because, as it was shown, changing the water vapor volume fraction from 4% to 16% increased the average heat transfer coefficient by more than a factor of two. The increase in the cooling water flow rate also had a similar effect on the total heat transfer. An analysis of inlet cooling water temperature variation showed that a temperature increase of approximately 5 °C reduced the condensate collection. The experimental results of the study of condensation heat transfer in six-stage heat exchangers connected in series are presented in [33]. The regularities of condensation of water vapor from the flue gas on vertical U-type inline tube bundles in a crossflow were analyzed. During the experiments, the flue gas flow rate was from 150 to 192 kg/h. It was found that as the temperature of the inlet cooling water increased, the condensation efficiency decreased almost linearly. The results showed that a cooling water temperature increase also affected condensation processes. If the cooling water temperature increased from ~24 °C to ~38 °C, the decrease in the condensation efficiency was from 75% to 46%. It was also observed that the first two stages of heat exchangers hardly collected any condensate, as they mainly worked to reduce the flue gas temperature, which was ~150 °C at the inlet to the test section. Most of the condensate formed in the fourth stage, and the condensate collection decreased in the fifth and sixth stages.

As we can see from the literature review, for vertical tube bundles in a crossflow, investigations are very limited, especially with a rather
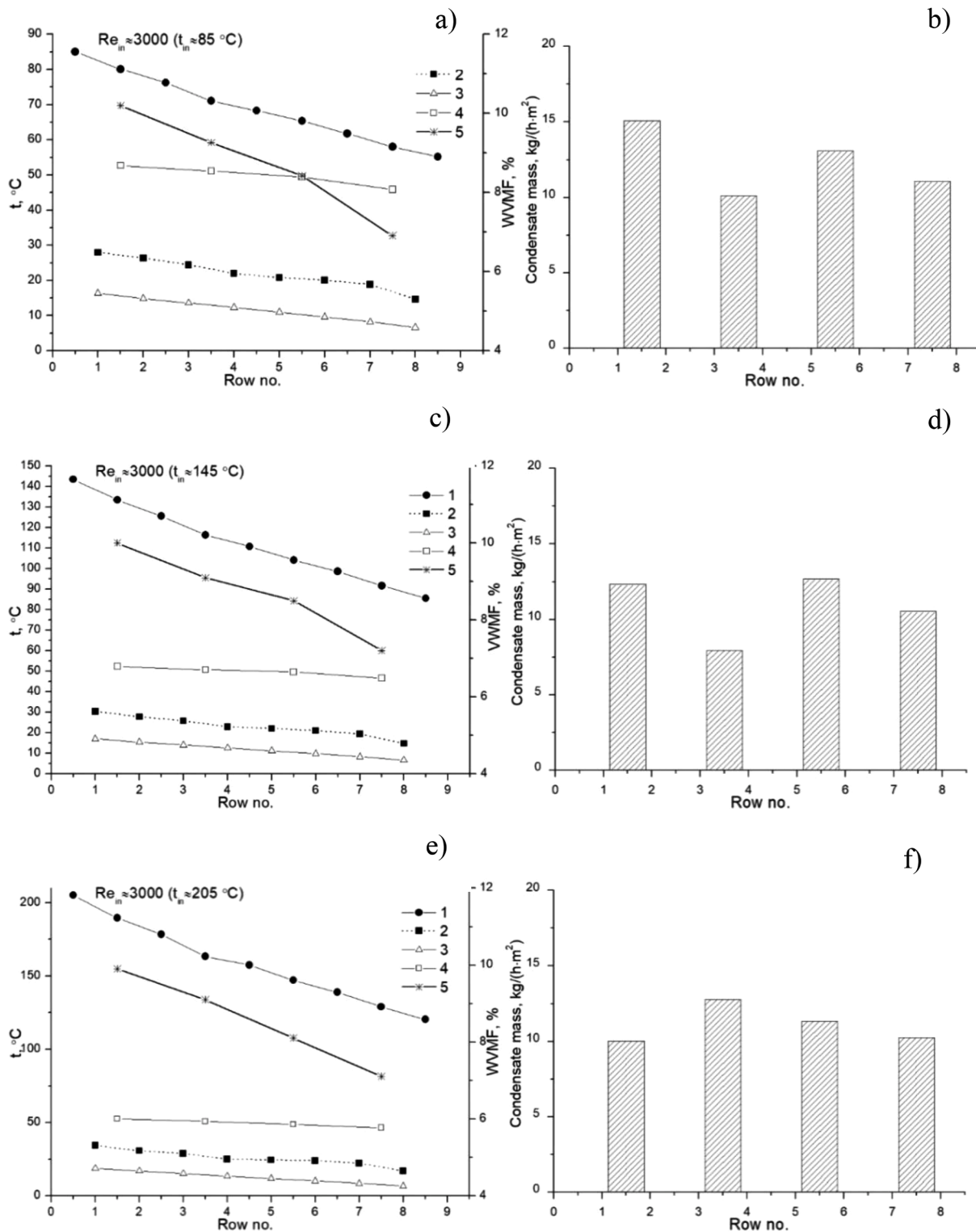
Fig. 2. Temperature, WVMF (a, c, e) and condensate mass variation (b, d, f) along the test section at Re_{in}=3000, t_{in}=85, 145, 205 °C. (1) average HA temperature, (2) average outside tube wall surface temperature, (3) cooling water temperature, (4) dew point temperature, (5) WVMF. *(2-column fittingimage).*

small water vapor mass fraction in non-condensable gasses. Therefore, this paper presents and discusses experimental results of total (convection and condensation) heat transfer in different rows of a vertical tube heat exchanger in a crossflow of humidified air (water vapor mass fraction 10% and 20%). The investigations were performed with the aim to determine the efficiency of a condensation heat exchanger and provide the quantification of the effects and the mapping of the distribution of heat transfer and condensate mass behavior in the bundle. This information on water vapor condensation in different rows of a heat exchanger from the practical industrial engineering point of view will provide an extended basis for the optimization of the design of heat exchangers for waste heat recovery. It also could be applied for the validation of computational models developed for condensation heat transfer and condensate flux numerical modeling along heat exchangers.
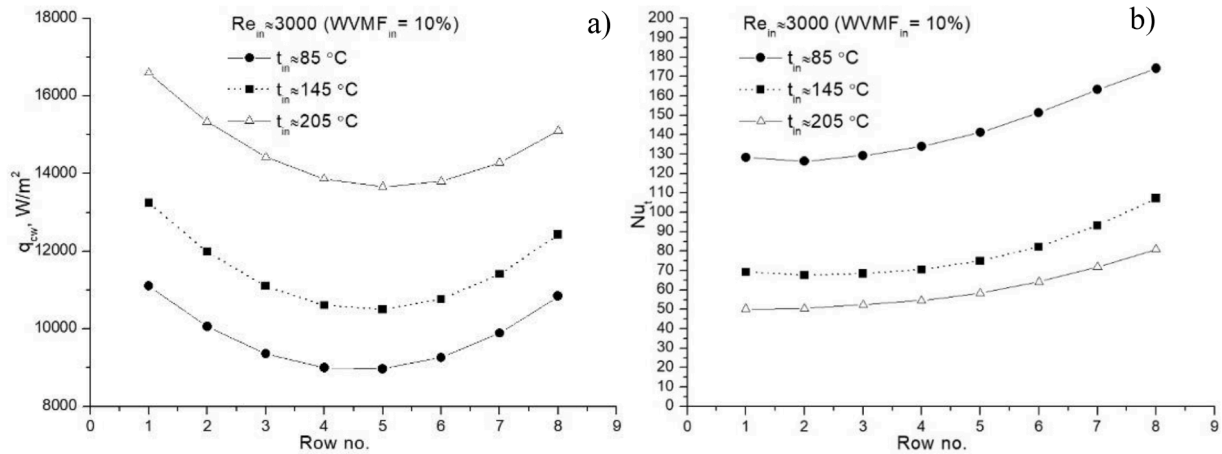
Fig. 3. Heat flux (a) and *Nu* number (b) variations along the test section at Re_{in}=3000 and different HA inlet temperatures.*(2-column fittingimage.)*.

In this study the investigations were performed at a fixed ratio of the cooling water and humidified air flow rate (it was kept to 3) and at a fixed cooling water inlet temperature (~7 °C), concentrating the attention on the effect of hot humidified gas parameter variation on the condensation process. In the future, it is necessary to extend these investigations to cover the cooling water parameter variation effect on the condensation heat transfer and condensate mass in different rows of a heat exchanger.

2. Experimental setup

The experimental setup with the test section used for the experiments is shown in Fig. 1. The main components of the experimental setup are the following: a heat exchanger (the test section), a compressor, air heaters, a steam generator and cooling water lines.

Air from the compressor (Kaeser, Germany) was supplied to the air heaters (Tutco, USA). The air passing the heaters was heated to the required temperature and flowed to the mixing chamber. Water vapor from the steam generator (Grundler, Germany) was also supplied to the mixing chamber. Then the humidified air (HA) was routed to the test section through the three-meter-long pipe.

The mixing chamber's length was 500 mm, and its outside diameter was also 500 mm. The chamber was connected to the three-meter-long pipe with an outside diameter of 270 mm.

During the experiments, the HA was supplied to the inlet of the test section. Flow rates of the air and water vapor were measured using flow rate meters (E + E Elektronik, Austria and Sierra Instruments, USA, accuracies ±3.3% and ±1.5%, respectively). The required water vapor mass fraction (WVMF) in the air being supplied to the test section was obtained by adjusting the flow rates of the air and water vapor. The WVMF was 10% and 20% during the experiments. At the outflow of the test section, the gas was directed to the stack and discharged to the atmosphere.

The test section used in the experiments was designed by the Lithuanian Energy Institute (LEI) in cooperation with Brunel University (London). The experiments were also performed at the LEI. The heat exchanger was composed of three longitudinal stainless-steel tubes of serpentine format (Ø18 × 2 mm), which were placed in a stainless-steel frame. The transverse pitch of the tube bundles was $a = 1.5$ and longitudinal pitch $b = 7.2$ (ratio $a/b = 0.2$). The total outer surface area of the tube bundles (i.e., heat transfer area) was about 0.49 m².

Cooling water for the test section was supplied from the municipal water supply system. After passing the test section, the cooling water was discharged into the sewage system. The cooling water and HA were flowing in counter-current directions. The cooling water flow was adjusted through each serpentine tube of the heat exchanger by valves,

and its flow rate was measured using water flow rate meters (Isomag, Italy, accuracy±0.4%).

The tube surface, HA and cooling water temperatures were measured using calibrated chromel-copel type thermocouples (wire diameter 0.2 mm, accuracy ±0.3%). All the thermocouple readings were collected using a Keithley automatic data acquisition system (accuracy ±0.25%).

The condensate was collected along the tube bundles in bottles at four positions (atrows no. 1&2, 3&4, 5&6 and 7&8, see Fig. 1). Every empty bottle before the experiment and the bottles with the condensate after the experiment were weighted on the scales (Beurer, accuracy ±1 g).

To avoid heat losses, the test section, the HA supply and the stack were insulated using Rockwool insulation. During all the experiments, the heat balance was checked. The error was calculated as Δ=[(Q$_f$-Q$_{cw}$)/ Q$_{cw}$]·100 and it was within 2–9%.

3. Methodology

Experiments were performed for three different inlet HA Reynolds numbers (Re_{in}= 3000, 5000, and 10,000), three inlet temperatures (85 °C, 145 °C, 205 °C) and two WVMFs (10% and 20%). The water vapor mass fraction in the released flue gasses depends on the fuel being incinerated. It can be in the range of 4–13% for coal, 10–15% for natural gas and up to 30% for biofuel [34–36]. Therefore, during this study two different WVMFs of 10% and 20% were selected.

All the experiments were performed at the pressure close to atmospheric. During the experiments, the ratio of the cooling water flow rate to the HA flow rate was kept at 3. The cooling water inlet temperature was ~7–8 °C during all the experiments.

The local parameters were calculated at 8 positions along the heat exchanger (represented by index i of the row in following formulas).

The specific heat flux obtained by the cooling water was determined as:

$$q_{t_i} = Q_{cw_i} \bigg/ S_i = \frac{m_{cwi}\left(c_{p_{i+1}} \cdot t_{cw,out,i} - c_{p_i} \cdot t_{cw,in,i}\right)}{\pi \cdot d \cdot l_i} \qquad (1)$$

where Q_{cw_i} is heat obtained by the cooling water, *W*; S_i is the outer surface area of the serpentine tubes, m²; m_{cwi} is the cooling water mass flow rate, kg/s; $c_p$is the specific heat of the water at outlet and inlet temperatures, kJ/(kg· °C); $t_{cw,in\text{-}out}$ are the temperatures of the cooling water at the inlet and outlet from each elbow of the tube, °C; d is the outer diameter of the tube, m; l is the length of the tube measured along the tube axis between the elbows of the tube, m.

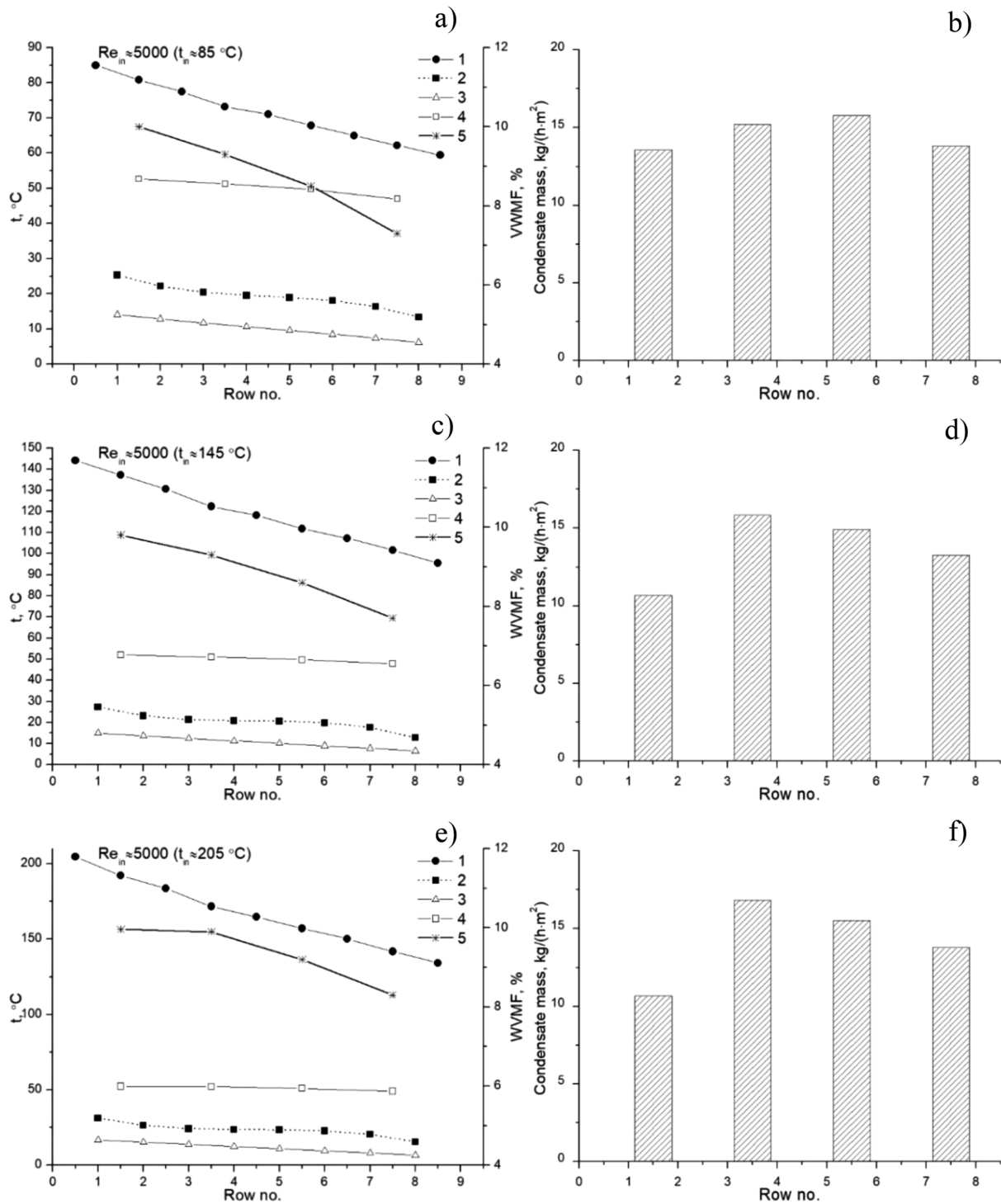Heat quantity released due to the HA cooling and water vapor condensation was obtained:

Fig. 4. Temperature, WVMF (a, c, e) and condensate mass variation (b, d, f) along the test section at Re_{in}=5000, t_{in}=85, 145, 205 °C. (1) average HA temperature, (2) average out side tube wall surface temperature, (3) cooling water temperature, (4) dew point temperature, (5) WVMF. *(2-column fittingimage)*.

$$Q_f = m_f \cdot \left(t_{f,in} \cdot c_{pf,in} - t_{f,out} \cdot c_{pf,out}\right) + m_{cd} \cdot r \qquad (2)$$

where m_f is the HA flow rate, kg/s; c_{pf} is the specific heat of the HA, kJ/(kg· °C); m_{cd} is the condensate flow rate, kg/s; r is latent heat of condensation, kJ/kg.

The total heat transfer coefficient (W/(m^2· °C)) for every row was calculated as follows:

$$\alpha_{t_i} = q_{t_i} \Big/ \left(t_f - t_w\right)_i \qquad (3)$$

where t_f is the average of the HA temperature measured at the center of the test section before and after a respective row, °C; t_w is the measured average outer tube wall temperature of the row, °C.

The total Nusselt number for each row:

$$Nu_{t_i} = \alpha_{t_i} \cdot d / \lambda_i \qquad (4)$$

where λ is the thermal conductivity of the HA based on t_f, W/(m· °C).

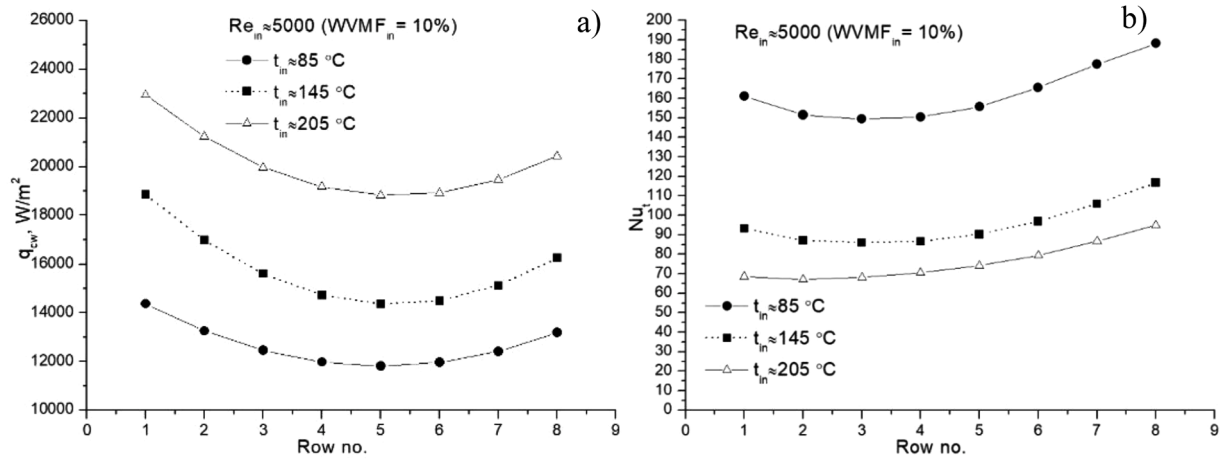Condensation efficiency was calculated according to the formula:

Fig. 5. Heat flux (a) and *Nu* number (b) variations along the test section when Re_{in}=5000 at different HA inlet temperatures. *(2-column fittingimage)*.

$$\eta = (m_{cd} / m_{v,in}) \cdot 100 \tag{5}$$

where m_{cd} is the total water condensate flow rate, kg/s, $m_{v,in}$ is the water (as vapor) flow rate at the inlet into the test section, kg/s.

Average heat transfer coefficient:

$$\overline{\alpha} = Q_{cw} / (S \cdot \Delta t_{ln}) \tag{6}$$

where Δt_{ln} is the logarithmic mean temperature, calculated as:

$$\Delta t_{ln} = \frac{(t_{f,in} - t_{cw,out}) - (t_{f,out} - t_{cw,in})}{\ln\left[(t_{f,in} - t_{cw,out})/(t_{f,out} - t_{cw,in})\right]} \tag{7}$$

Average Nusselt number:

$$\overline{Nu} = \overline{\alpha} \cdot d / \lambda \tag{8}$$

In this formula, thermal conductivity λ was evaluated based on the average HA temperature $\overline{t} = (t_{f,in} + t_{f,out})/2$.

Calculation of the HA inlet Reynolds number is based on formula:

$$Re_{in} = \frac{G_{f,in} \cdot d \cdot \rho_{f,in}}{S_{min} \cdot \mu_{f,in}} \tag{9}$$

where $G_{f,in}$ is the volumetric HA flow rate, m^3/s; S_{min} is the minimal flow area between the tubes, m^2; $\rho_{f,in}$ is the HA density at the inlet to the test section, kg/m^3 and $\mu_{f,in}$ is the HA dynamic viscosity at the inlet to the test section, kg/(m·s). Parameters in formula 8 are calculated based on the HA inlet temperature.

Calculation of the HA outlet Reynolds number is based on formula:

$$Re_{out} = \frac{G_{f,out} \cdot d \cdot \rho_{f,out}}{A_{min} \cdot \mu_{fout}} \tag{10}$$

The HA average *Re* number is calculated as:

$$\overline{Re} = \frac{Re_{in} + Re_{out}}{2}. \tag{11}$$

The local WVMF was calculated based on the local HA flow rate (collected condensate flow rate was excluded). Local dew point temperatures were calculated based on the local WVMF and its temperature, using formulas presented in [37].

Saturation vapor pressure:

$$p_s = \left(6,089,613 \cdot 10^{\frac{7.33.502 \cdot t_f}{230.3921 + t_f}}\right) \cdot 100 \tag{12}$$

Water vapor pressure:

$$p_{H2O} = p_s \cdot \frac{RH}{100} \tag{13}$$

Absolute humidity:

$$AH = \frac{2.1667 \cdot p_{H2O}}{t_f + 273.15} \tag{14}$$

Dew point temperature:

$$t_d = \frac{230.3921}{\left(\frac{7.33502}{\log_{10}\left(\frac{p_{H2O}}{6.08961}\right)}\right) - 1} \tag{15}$$

4. Results and discussion

4.1. Water vapor mass fraction (WVMF) 10%

Reynolds number 3000. Fig. 2 presents local distributions of temperatures, WVMFs and collected condensate mass variation along the test section when the HA Reynolds number (Re_{in}) was 3000 and the HA inlet temperatures (i.e., temperatures before the first row of tubes) were 85 °C, 145 °C and 205 °C.

Temperature variation in the test section (Fig. 2a, c, e, curve1) at all the HA inlet temperatures had the same profile, i.e., the HA temperature was constantly decreasing from the inlet (at row no. 1) to the outlet (at row no. 8), the cooling water temperature (Fig. 2a, c, e, curve 3) was increasing from the inlet (at row no. 8) to the outlet (at row no. 1) and the tube surface temperature was higher than the cooling water temperature but repeated its variation.

With an increase in the HA inlet temperature, the temperatures in the test section also increased, and therefore the difference between the HA temperature and the tube wall surface temperature became bigger. The results also indicate that the dew point temperature (Fig. 2a, c, e, curve 4) slowly decreased from about 53 °C at the inlet along the test section up to the outlet.

In any case, at the outlet from the test section, the WVMF decreased to 6.8%. Therefore, in general the change (decrease) in the WVMF throughout the test section was about 3%. A similar tendency was also evident for the dew point temperature as it was closely related to the WVMF.

For all the cases presented in Fig. 2a, c, e, it can be seen that the dew point temperature in the test section at all times remained higher than the tube wall surface temperature, and therefore condensation should be present at all the rows of the test section. This was confirmed by the results of the condensate collection (Fig. 2b, d, f). The results indicated that condensation was present in all the rows. However, the collected condensate mass varied along the test section. At lower HA inlet temperatures (85 °C and 145 °C), a rather intensive condensing process was
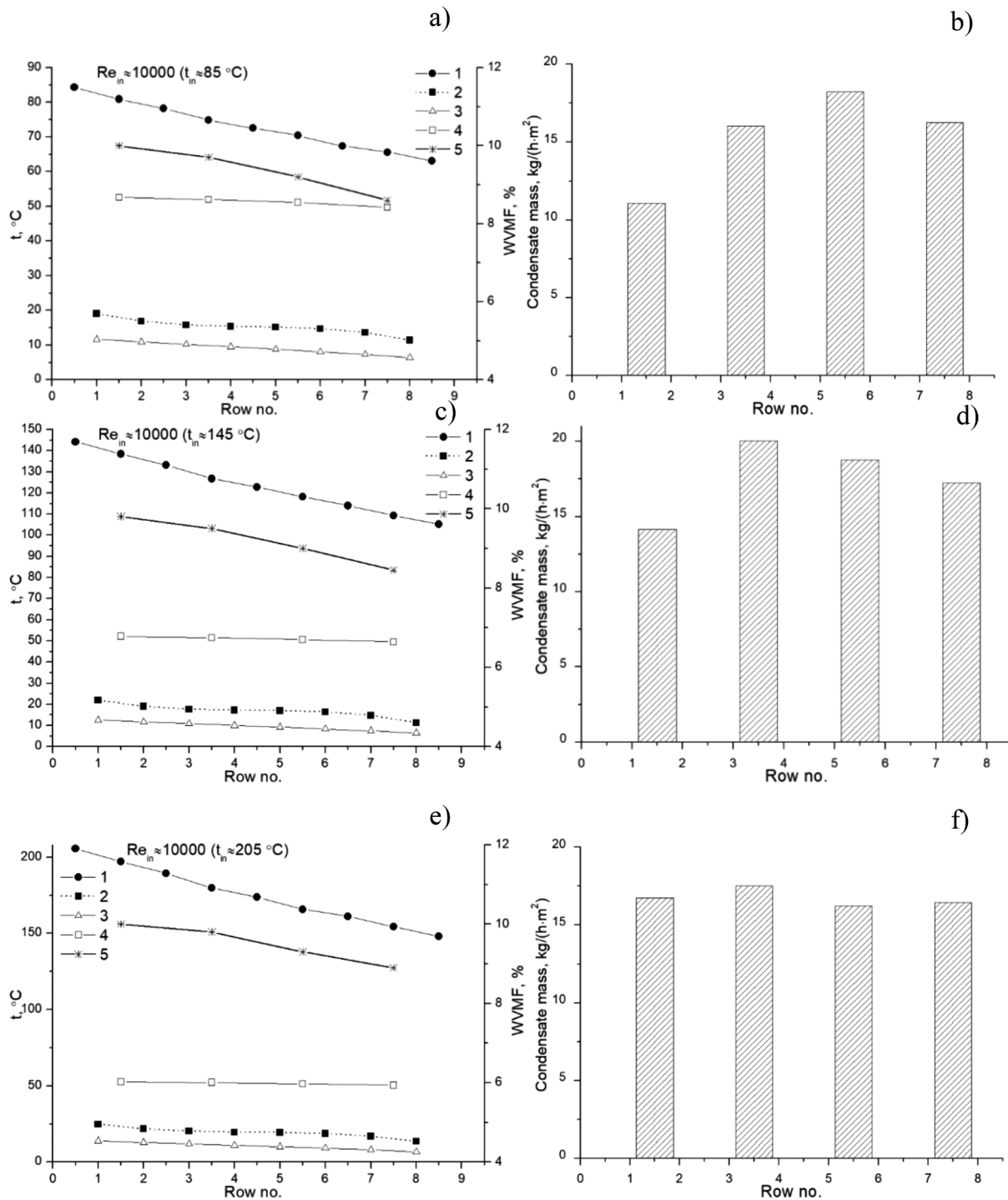
Fig. 6. Temperature, WVMF (a, c, e) and condensate mass variation (b, d, f) along the test section at Re_{in}=10,000, t_{in}=85, 145, 205 °C. (1) average HA temperature, (2) average outside tube wall surface temperature, (3) cooling water temperature, (4) dew point temperature, (5) WVMF.*(2-column fitting image)*.

observed at the beginning of the test section (rows no. 1&2) with further variation along the remaining part of it. The profile of the collected condensate mass for these HA inlet temperature cases (Fig. 2b, d) was very similar, but the absolute values of the collected condensate mass in the case of a higher HA inlet temperature (145 °C) was smaller than those obtained when the HA inlet temperature was 85 °C.

The profile of condensate mass variation along the test section was different for the highest HA inlet temperature (205 °C) in comparison with the lower ones (85 °C and 145 °C). Here (Fig. 2f), the maximum of the condensate mass collected shifts further from the beginning of the

test section, i.e., to rows no. 3&4.

Collected condensate mass results show (Fig. 2b, d, f) that the mass in the rows along the heat exchanger in comparison with the average value was varying in the range between 10% and 20%. The higher the temperature (HA inlet temperature), the narrower the varying range.

Distributions of the heat fluxes (i.e., q_{cw}=q_t) and the total *Nu* numbers along the test section are presented in Fig. 3. The variation of the heat fluxes along the test section for all three HA inlet temperatures is similar (Fig. 3a). The highest heat flux is at the beginning of the test section for all the HA inlet temperatures. The collected condensate mass
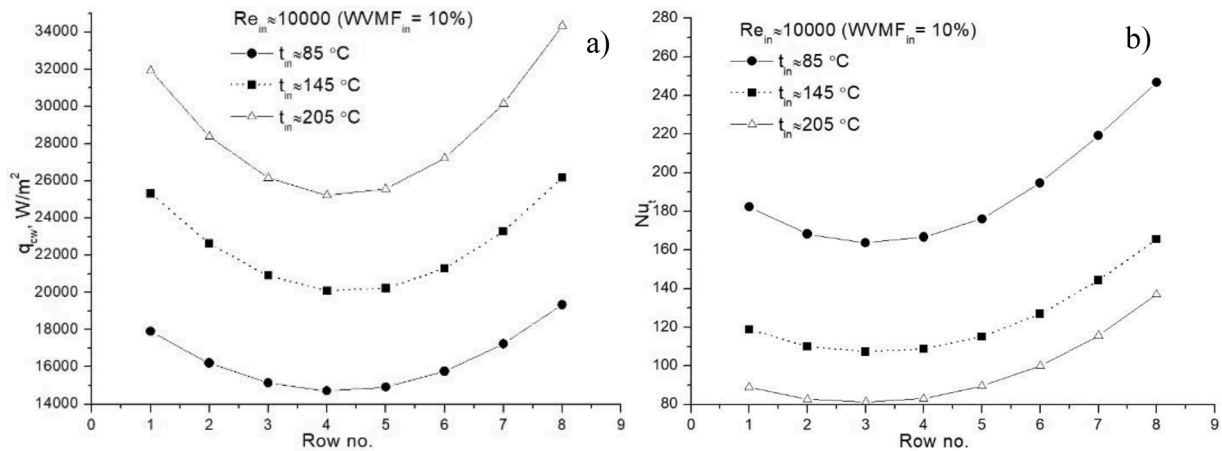
Fig. 7. Heat flux (a) and *Nu* number (b) variationsalong the test section when Re_{in}=10,000 at different HA inlet temperatures. *(2-column fitting image)*.

(Fig. 2b) in all the rows is similar, and therefore, due to a large temperature difference between the HA and cooling water temperatures, the convection heat flux is prevailing here. Further, as the HA temperature difference along the test section is decreasing (Fig. 2), the influence of the convection heat transfer is decreasing, and thus the heat flux is decreasing as well and reaches its minimum value at rows no. 4&5. Cold water at the inlet stipulates the increase in the heat fluxes from rows no. 6–8. As we can see from Fig. 3a, with the increase in the HA inlet temperature, the heat flux also increases significantly. This is caused by the increased heat transfer by convection due to a significant increase in the temperature difference between the HA and tube wall, when the condensation heat transfer is decreasing with the increase in the HA inlet temperature (Fig. 2b).

The variation of the *Nu* number along the test section (Fig. 3b) is different in comparison with the variation of the heat flux as the *Nu* number takes into account the temperature difference between the HA and the tube wall. For all the cases, the total Nu number increases along the heat exchanger.

The profile of the total Nu number variation along the test section was very similar for all three HA inlet temperatures and the graphical curves lay almost parallel to each other. The results in general indicate that at higher HA inlet temperatures we get a smaller Nu_t due to a larger temperature difference between the HA and the tube wall. At the HA inlet temperatures of 145 °C and 205 °C, the Nu_t decreased by factors of about 1.8 and 2.6, respectively, compared to the Nu_t obtained at 85 °C. Despite that, the Nu_t remained rather high, i.e., in the range between 50 and 80, even at the highest HA inlet temperature (205 °C). The increase in the Nu_t along the test section was due to a decreasing temperature difference between the HA and the tube wall.

The results in general indicate (Fig. 3b) that better conditions for condensation and a higher Nu$_t$ along the test section are achieved at a lower HA inlet temperature. A higher HA inlet temperature had a deteriorating effect on condensation and the Nu_t.

Fig. 4 presents local distributions of temperatures, WVMFs and collected condensate mass variation along the test section at a higher HA inlet Reynolds number (*Rein*) than presented in Fig. 2, but at the same HA inlet temperatures (85 °C, 145 °C and 205 °C).

Reynolds number 5000. The distribution of temperatures along the test section (Fig. 4a, c, e) at *Rein*=5000 is very similar to those presented in Fig. 2 at *Rein*=3000. However, it should be noted that at *Rein*=5000, the HA temperature decrease along the test section (Fig. 4a, c, e, curve 1) was smaller in comparison to that at *Rein*=3000. The profiles and the values of cooling water and tube wall surface temperatures (Fig. 4a, c, e, curve 3 and 2) along the test section in this case were almost the same as the ones obtained for the lower *Rein*.

The change in the dew point temperature (Fig. 4a, c, e, curve 4) was

more pronounced at the HA inlet temperature of 85 °C, and along the test section, the dew point temperature decreased by about 6 °C, i.e., from 53 °C to ~ 47 °C. When the HA inlet temperature was higher (145 °C and 205 °C), the decrease in the dew point temperature was less pronounced.

The WVMF (Fig. 4a, c, e, curve 5) also decreased more evidently when the HA inlet temperature was 85 °C. Here, the difference between the WVMF at the inlet and the outlet of the test section is almost 3% (i.e., decrease from 10% to about 7%). With an increasing HA inlet temperature (145 °C and 205 °C), the decrease in the WVMF along the test section became smaller.

For all the HA inlet temperatures, the dew point temperature (Fig. 4a, c, e, curve 4) also remained higher than the tube wall surface temperature (Fig. 4a, c, e, curve 3), and therefore condensation took place in all the rows of the heat exchanger (Fig. 4b, d, f). The variation of the condensate mass collected along the test section was very similar for all the HA inlet temperatures. The biggest changes were noticed at rows no. 1&2, where the increasing HA inlet temperature resulted in a decrease in the condensate mass collected. The maximum condensate mass at t_{in}=85 °C was obtained at rows no. 5&6. At higher temperatures (t_{in}=145 °C and 205 °C), it was at rows no. 3&4.

The condensate mass in the rows along the heat exchanger (Fig. 4b, d, f) varied in the range between 10% and 25% in comparison with the average value.

Distributions of the heat fluxes presented in Fig. 5a show similar tendencies as obtained for the lower HA inlet Reynolds number (Fig. 3a). The only difference is that at Re_{in}=5000, the heat fluxes are larger and the minimums are shifted further, i.e., to rows no. 5&6 in comparison with the results obtained at Re_{in}=3000.

At the beginning of test section, due to a large temperature difference between the HA and cooling water temperatures, the convection heat flux prevails. Further, as the HA temperature difference along the test section decreases (Fig. 4), the influence of the convection heat transfer also decreases, and thus, the heat flux decreases until it reaches its minimum value at rows no. 5&6. Cold water at the inlet stipulates the increase in the heat fluxes from rows no. 6–8. As we can see from Fig. 5a, with the increase in the HA inlet temperature, the heat flux also increases, and such an increase is due to the increased heat transfer by convection because of the significant increase in the temperature difference between the HA and the tube wall.

The profile of the Nu_t variation for different inlet temperatures presented in Fig. 5b shows that Nu$_t$ decreased with the increasing HA inlet temperature. In general, the behavior of the Nu_t along the test section in this case was also similar to that determined for Re_{in}=3000 (Fig. 3). The increase in the Re_{in} to 5000 (i.e., the increase in the HA velocity) resulted in bigger local Nu_t values in comparison to those determined at
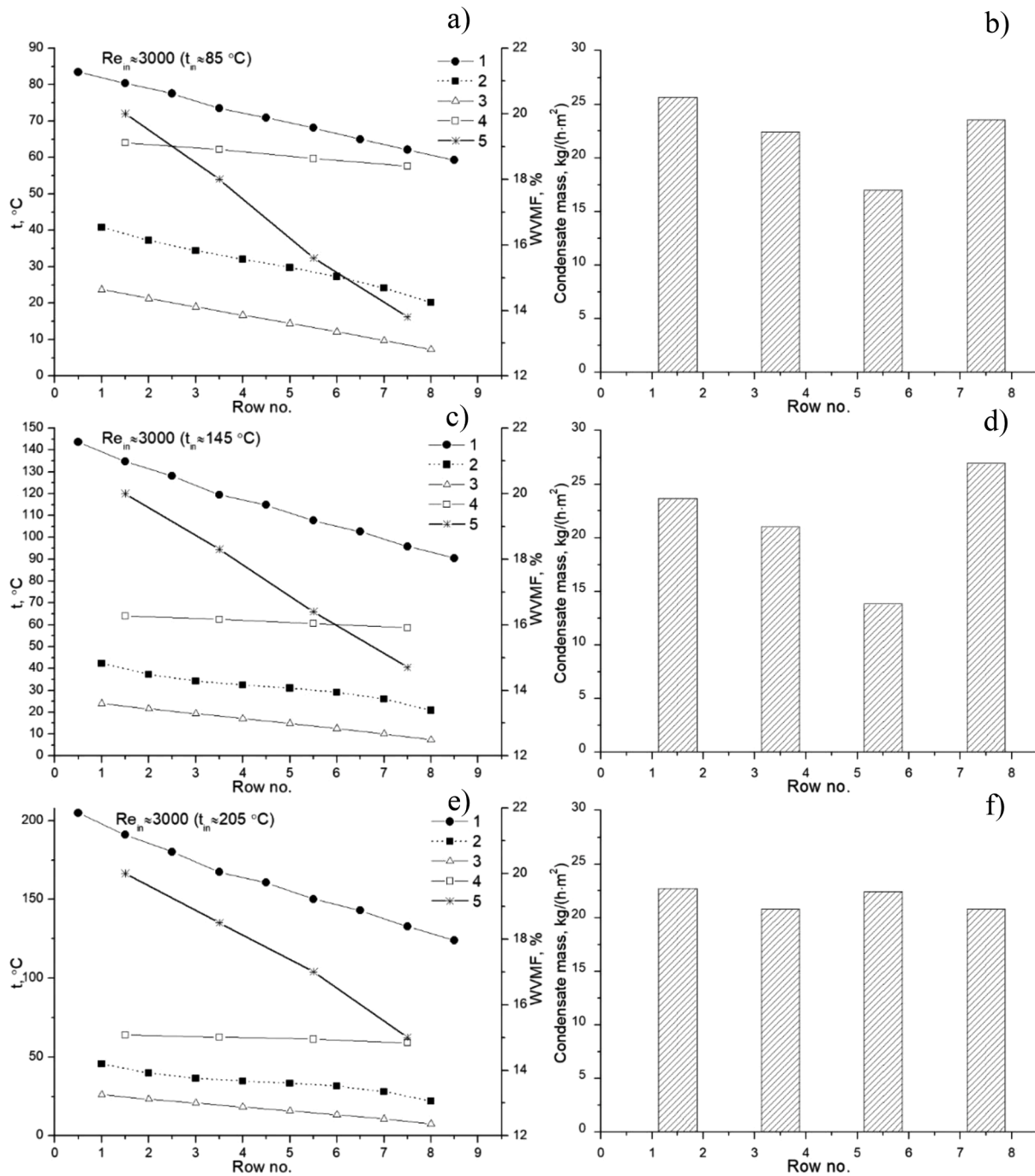
Fig. 8. Temperature, WVMF (a, c, e) and condensate mass variation (b, d, f) along the test section at Re_{in}=3000, t_{in}=85, 145, 205 °C. (1) average HA temperature, (2) average outside tube wall surface temperature, (3) cooling water temperature, (4) dew point temperature, (5) WVMF. *(2-column fitting image)*.

Re_{in}=3000.

Reynolds number 10,000. The temperature, WVMF and condensate mass variation for the highest Re_{in} number (10,000) used during the experiments are presented in Fig. 6. The highest Re_{in} means the biggest HA velocity through the test section and, thus, less time for the HA to spend in the heat exchanger before its discharge to the atmosphere. However, despite these changes, the results obtained for the temperature variations along the test section were the same as for the earlier cases (Fig. 6a, c, e).

The decrease in the WVMF (Fig. 6a, c, e, curve 5) from the inlet up to the outlet of the test section was also rather small, about 1.4% and 1.1% for the lowest and the highest HA inlet temperatures, respectively. This, of course, resulted in small changes in the dew point temperature along

the test section (Fig. 6a, c, e, curve 4), which was in the range of about 53–50 °C.

The tube surface temperature remained below the dew point temperature all the time, and hence condensation was present in all the rows (Fig. 6b, d, f). The profile of the collected condensate for the cases when the HA inlet temperatures were 85 °C and 145 °C was similar, with pronounced minimums and maximums in certain rows (Fig. 6b, d). At the highest HA inlet temperature (205 °C), the collected condensate mass was almost equal in all the rows, and it was in the range between 16 and 17.5 kg/(h·m²).

The condensate mass in the rows along the heat exchanger (Fig. 4b, d, f) in comparison with the average value varied in the range between 15 and 30% when t_{in} = 85–145 °C and between 5 and 7% when t_{in} = 205
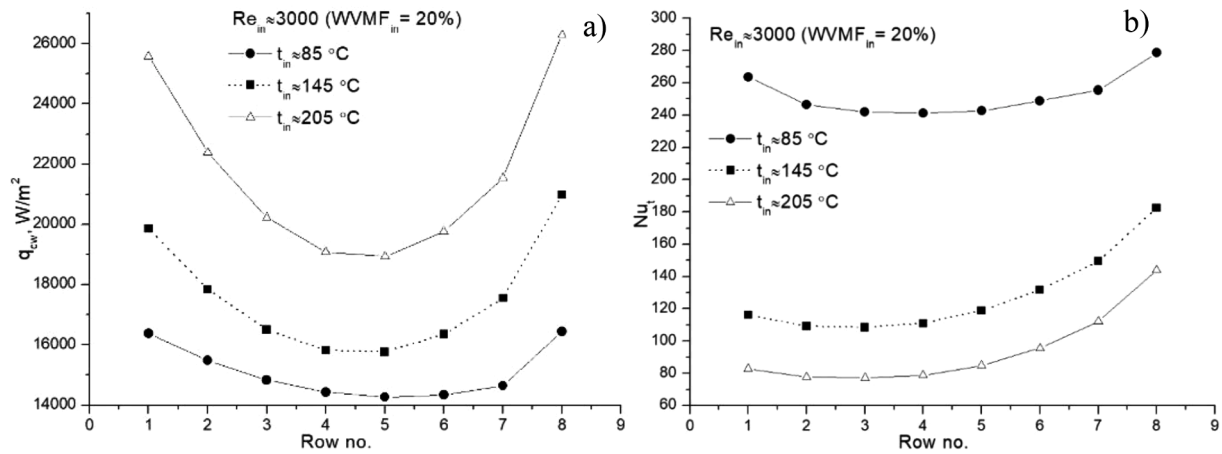
Fig. 9. Heat flux (a) and *Nu* number (b) variations along the test section when Re_{in}=3000 at different HA inlet temperatures. *(2-column fitting image)*.

°C.

The characters of heat fluxes along the test section (Fig. 7a) are similar to those already discussed for smaller HA inlet Reynolds numbers. It is evident that with an increase in the Re_{in} number, the heat fluxes also increase.

The Nu_t numbers (Fig. 7b) were rather similar to those determined at the smaller Re_{in} numbers. However, at Re_{in}=10,000, the Nu_t had a clear minimum at row no. 3 for all HA inlet temperatures. It should be noted that Nusselt number values are defined by the heat flux as well as by the difference between the HA and tube wall surface temperatures, and therefore this causes smaller Nusselt numbers for higher temperatures of the HA.

Distributions of the Nu_t are almost parallel along the test section for all HA inlet temperatures. An increase in the temperature by 60 °C (from 85 °C to 145 °C) resulted in a Nu_t decrease by a factor of about 1.5, and an increase in the temperature by 120 °C (from 85 °C to 205 °C) decreased the Nu_t by about a factor of 2.

4.2. Water vapor mass fraction (WVMF) 20%

Experiments with the WVMF of 20% were performed in order to investigate the condensation dependency on water vapor mass fraction in the HA. The investigations were conducted keeping similar conditions as presented in the previous subsection (i.e., HA inlet Reynolds numbers, temperatures, and cooling water flow rates).

Reynolds number 3000. The experimental results with the WVMF of 20% are presented in Fig. 8. Although HA inlet and cooling water temperatures were the same as during the experiments with the WVMF of 10% (Fig. 2a, c, e), the results show that the decrease in the HA temperature along the test section was smaller and the increase in the cooling water temperature was bigger when the WVMF was 20% (Fig. 8a, c, e). In general, the distribution characteristics of the HA, cooling water and tube wall surface temperatures were similar to the profiles for the WVMF of 10%.

The results also indicate that with an increase in the HA inlet temperature, the dew point temperature (Fig. 8a, c, e, curve 4) decreased less along the test section from the inlet up to the outlet. This is related to the WVMF, which shows the same (decreasing) tendency with an increasing HA inlet temperature (Fig. 8a, c, e, curve 5). For example, when t_{in} = 85 °C, the decrease in the WVMF is about 6.2% (from 20% to 13.8%), when t_{in} = 145 °C, the decrease in the WVMF is by about 5.5% (from 20% to 14.5%) and when t_{in} = 205 °C, the decrease is about 5%.

As the WVMF in this case was 20%, the dew point temperature was higher than at the WVMF of 10% and was well above the tube wall surface temperature. Therefore, condensation was present in all the rows of the test section, and the condensate mass collected was greater

than with the WVMF of 10% (cf. Fig. 8b, d, f and Fig. 2b, d, f). The distribution of the condensate mass was not very uniform in the rows along the heat exchanger.

The condensate mass in the rows along the heat exchanger (Fig. 8b, d, f) in comparison with the average value varied in the range between 10% and 35% when t_{in} = 85 °C or 145 °C and between 3% and 5% when t_{in} = 205 °C.

The variations of the heat fluxes presented in Fig. 9a are similar to those obtained in the case of the smaller WVMF; however, the absolute values are much larger. In this case, the highest heat flux is also at the beginning of the test section for all the HA inlet temperatures. Due to a large temperature difference between the HA and cooling water temperatures, the convection heat flux prevails. Further, as the HA temperature difference along the test section decreases (Fig. 8), the influence of the convection heat transfer decreases, and thus, the heat flux decreases until it reaches it minimum value at rows no. 4&5. Cold water at the inlet stipulates the increase in the heat fluxes from rows no. 5–8. The results show (Fig. 9a) that with an increase in the HA inlet temperature, the heat flux increases significantly.

The characteristic of the local total Nusselt number variation at t_{in} = 85 °C (Fig. 9b) differs slightly from that obtained when the WVMF was 10% (Fig. 3b). At higher HA temperatures (145 °C and 205 °C), the characteristic of the Nu_t for both WVMFs was practically the same. The increase in the WVMF to 20% influenced the Nu_t and increased it noticeably, i.e., at least by a factor of about 1.6 in comparison to the WVMF of 10%.

Reynolds number 5000. In general, the temperature distributions and WVMF results at Re_{in}=5000 (Fig. 10a, c, e) were typical of those discussed earlier, with some minor differences in the temperature or WVMF values. The distribution of the condensate mass collected (Fig. 10b, d, f) did not show any dramatic changes in comparison with the previously discussed results.

Condensation in the rows along the heat exchanger was rather even, with a variation of about 5–10% from the average value.

The heat fluxes presented in Fig. 11a show similar tendencies to those already discussed for Re_{in}=3000.

The Nu_t distribution along the test section (Fig. 11b) was similar to that presented for Re_{in}=3000 (Fig. 9b), except for the case at t_{in} = 85 °C (Fig. 11b), where, at the beginning of test section, the Nu_t is smaller in comparison with the case at Re_{in}=3000 (Fig. 9b). A comparison of the Nu_t at Re_{in}=5000 and at the WVMFs of 10% and 20% shows that for the latter case, the Nu_t is much higher, and this is especially evident at the lowest HA inlet temperature (t_{in} = 85 °C).

Reynolds number 10,000. In the case of Re_{in}=10,000, the HA temperature decrease (Fig. 12a, c, e, curve 1) along the test section is slightly smaller and the increase in the cooling water temperature
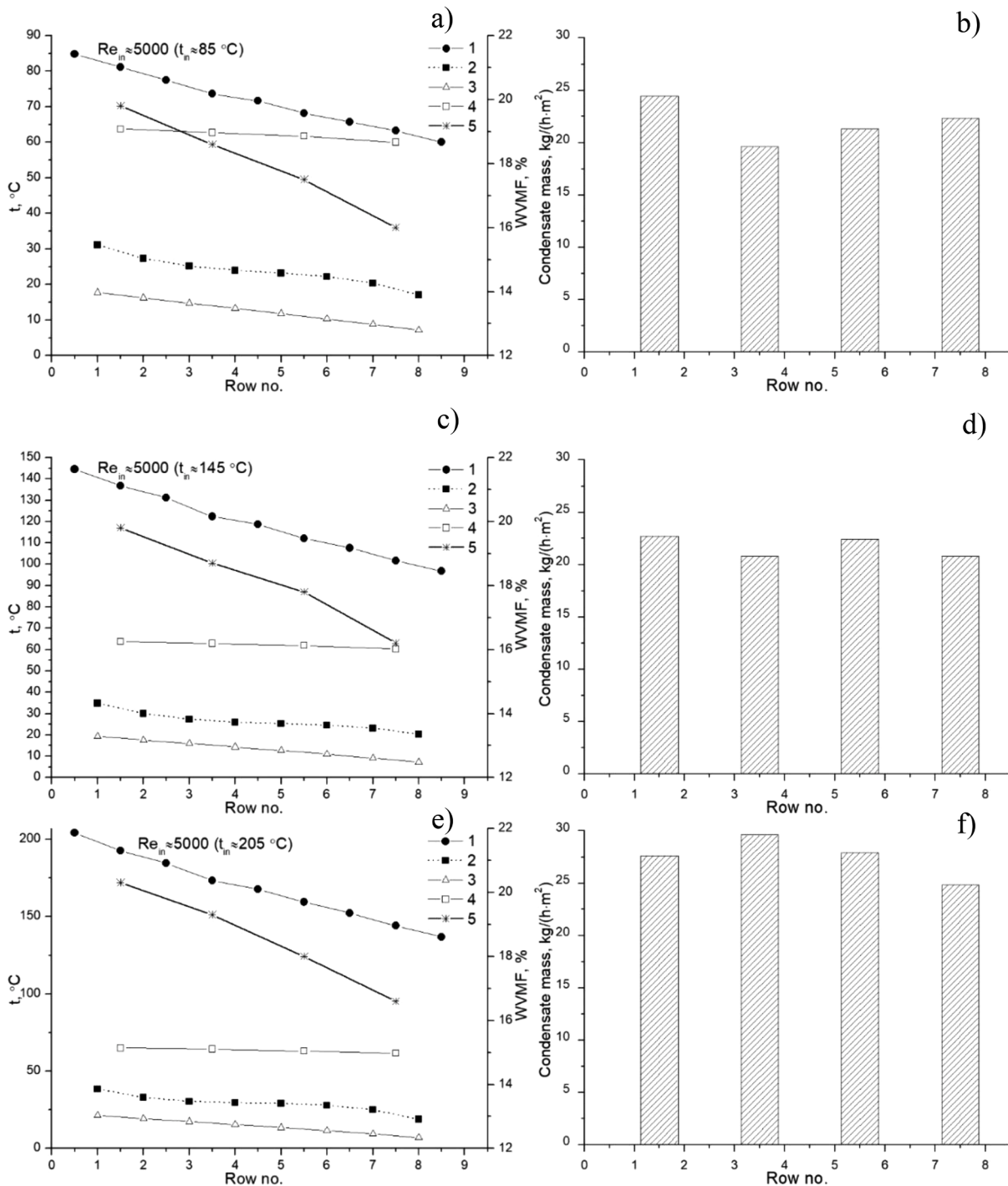
Fig. 10. Temperature, WVMF (a, c, e) and condensate mass variation (b, d, f) along the test section at Re_{in}=5000, t_{in}=85, 145, 205 °C. (1) average HA temperature, (2) average outside tube wall surface temperature, (3) cooling water temperature, (4) dew point temperature, (5) WVMF. *(2-column fitting image)*.

(Fig. 12a, c, e, curve 3) is slightly bigger in comparison with the results at the smaller WVMF for the same Re_{in} number (Fig. 6a, c, e).

The main difference between this case and all the previous results is that the tube surface wall temperature, especially for the cases when t_{in}=85 °C and 145 °C, does not have pronounced minimums and maximums along the test section (Fig. 12a, c, e, curve 2).

For all the HA inlet temperatures, the collected condensate mass was the biggest in rows no. 1&2 and 3&4 (Fig. 12b, d, f). The variation in condensation in the rows along the heat exchanger was also about 5–10% from the average value.

The heat fluxes obtained by the cooling water (Fig. 13a) are typical in

profile to those determined at smaller Re_{in} numbers.

The total local Nu_t number based on the local heat flux and the temperature difference between the HA and the tube wall surface is shown in Fig. 13b. When t_{in}=85 °C, there was a clearly pronounced minimum at rows no. 3&4. After that, the Nu_t increased and at the end of test section it even exceeded the Nu_t determined at the beginning of the test section. In this case, the Nu_t was rather high along the test section and varied between 300 and 380 and was much higher (in comparison with the results at the WVMF of 10% (Fig. 7b).

The increase in the HA inlet temperature, as already discussed, gave the same result, i.e., a decrease in the Nu_t. However, even for the biggest
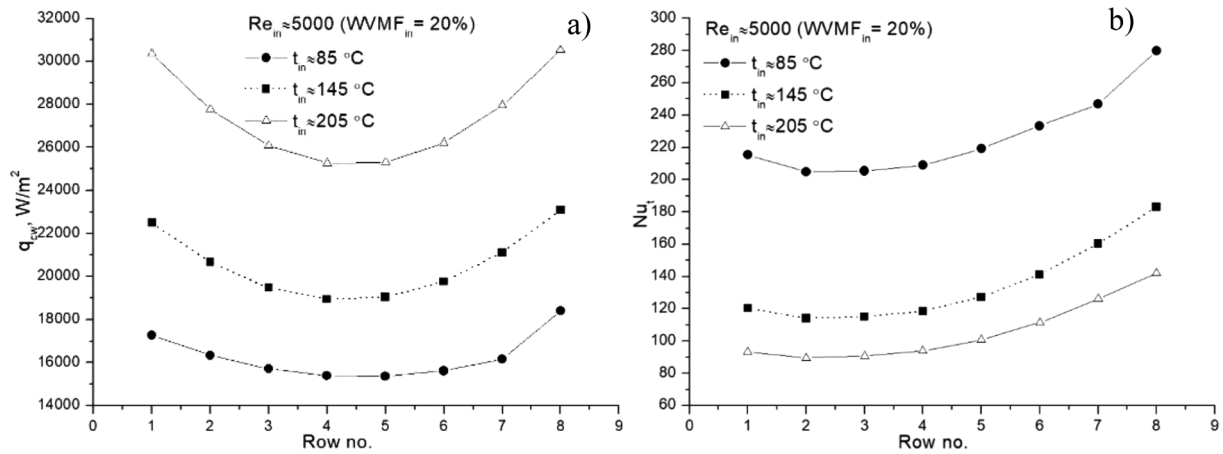
Fig. 11. Heat flux (a) and Nu number (b) variationsalong the test section when Re_{in}=5000 at different HA inlet temperatures. *(2-column fitting image)*.

HA inlet temperature, the Nu_t remained above 120, which was still almost 1.5 times bigger in comparison to the Nu_t obtained in the case of the WVMF of 10%.

4.3. Comparison of the results for different inlet WVMFs and temperatures

A comparison of the average $\overline{Nu}$ number at different HA average Reynolds numbers using the logarithmic temperature differences of this study with the average Nusselt number for dry air is presented in Fig. 14. The average $\overline{Nu}$ number for dry air in the turbulent Re number region was calculated using equation [39]:

$$\overline{Nu}_{dry-air} = 0.27 \cdot \overline{Re}^{0.63} \cdot Pr^{0.36} \cdot (Pr/Pr_w)^{0.25} \tag{16}$$

where Pr/Pr_w is the ratio of the Prandtl number of the bulk of humidified air to the Prandtl number at the wall which can be ignored in the above formula because the HA properties do not change dramatically at the wall during the experiments.

According to the above formula, the average $\overline{Nu}$ number obtained in the case of dry air for $\overline{Re}$ =3000, 5000 and 10,000 is 36.8, 50.8 and 78.6, respectively.

The results (Fig. 14) show that even a small WVMF (10%) enhances the average Nu number in comparison with the dry air $\overline{Nu}$ number. The results presented in Fig. 14 also indicate that the average $\overline{Nu}$ number dependence on the $\overline{Re}$ for dry air and HA is similar.

In the case of the WVMF of 10%, the average $\overline{Nu}$ number in comparison with the dry air $\overline{Nu}$ number increases by a factor of 1.2–3, and in the case of the WVMF of 20%, it increases by a factor of 1.7–5.

With the increase in the WVMF from 10% to 20%, the increase in the heat transfer is by a factor of 1.4–1.8. So, in general these results correlate rather well with the data presented in [31], where with the increase in the water fraction from 4% to 16%, the heat transfer increased by a factor of two.

For both WVMF cases (Fig. 14), the HA temperature has negative effect on the $\overline{Nu}$, i.e., the higher the temperature, the bigger the decrease in the $\overline{Nu}$observed. The uncertainties for the Nusselt number were evaluated using the methodology presented in [38]. The highest uncertainties are at the end of the test section, where the temperature difference between the HA temperature and the tube wall temperature is the smallest. These uncertainties are between 5 and 9%.

Based on the analysis of the results, a correlation for calculation of the average $\overline{Nu}$ number due to condensation was proposed:

$$\overline{Nu} = 6.7 \cdot WVMF^{1.48} \cdot t_{in}^{-\left(0.46 \cdot WVMF^{0.22}\right)} \cdot Re^{0.35} \tag{17}$$

The formula is valid when the HA Re_{in} number is in the range between 3000 and 10,000, the HA inlet temperature is in the range between 85 °C and 205 °C, the inlet water vapor mass fraction varies between 10–20%, the cooling water inlet temperature is 7–8 °C, and the ratio of the cooling water flow rate to the HA flow rate equals 3. The maximum relative error between the experimentally obtained average $\overline{Nu}$ number and the $\overline{Nu}$ number calculated by formula is up to 10%, the correlation coefficient is 0.978.

In the next figure (Fig. 15), a comparison is presented for the condensation efficiencies for both inlet WVMFs for different HA Reynolds numbers and temperatures. In general, the results show that with an increase in the HA inlet temperature, the condensation efficiency decreases. The same is true for the HA Re_{in} number because the higher Re_{in} number means that the HA spends less time in the heat exchanger, and hence the condensation efficiency is lower.

For the WVMF equal to 10%, the condensation efficiency reached almost 45% at the smallest Re_{in} number and the smallest HA inlet temperature. At higher HA inlet temperatures, the condensation efficiency was lower, about 35%. An increase in the Reynolds number to 5000 resulted in a noticeable condensation efficiency decrease, while at Re_{in}=10,000 there was a further significant decrease; for all three inlet temperatures it was between 15 and 20%.

In the case of the WVMF equal to 20%, the condensation efficiency at Re_{in}= 3000 and inlet temperatures of 85 °C and 205 °C was practically the same as in the case of the WVMF equal to 10%. At Re_{in}=5000, there was a sharp decrease in the condensation efficiencies for all inlet temperatures, and the efficiencies at all the inlet temperatures were almost the same, i.e., they decreased by about 25%. A further increase in the Reynolds number to 10,000 resulted in only a small condensation efficiency decrease by about 20–25%, and therefore it remained higher than it was in comparison with the WVMF of 10% (~15–20%).

5. Conclusions

The results of the investigations performed lead to the following conclusions:

1. Water vapor condensation was detected in all rows along the heat exchanger for all humidified air temperatures (85–205 °C). This happened because in all cases, the tubes' surface temperatures were always lower than the dew point temperature of the humidified air.
2. In the cases with a higher water vapor mass fraction (WVMF) (20%) and a higher humidified air inlet temperature, the condensation was rather even, with a variation of 5–15% from the average value. In the cases of a smaller WVMF (10%) and lower humidified air inlet
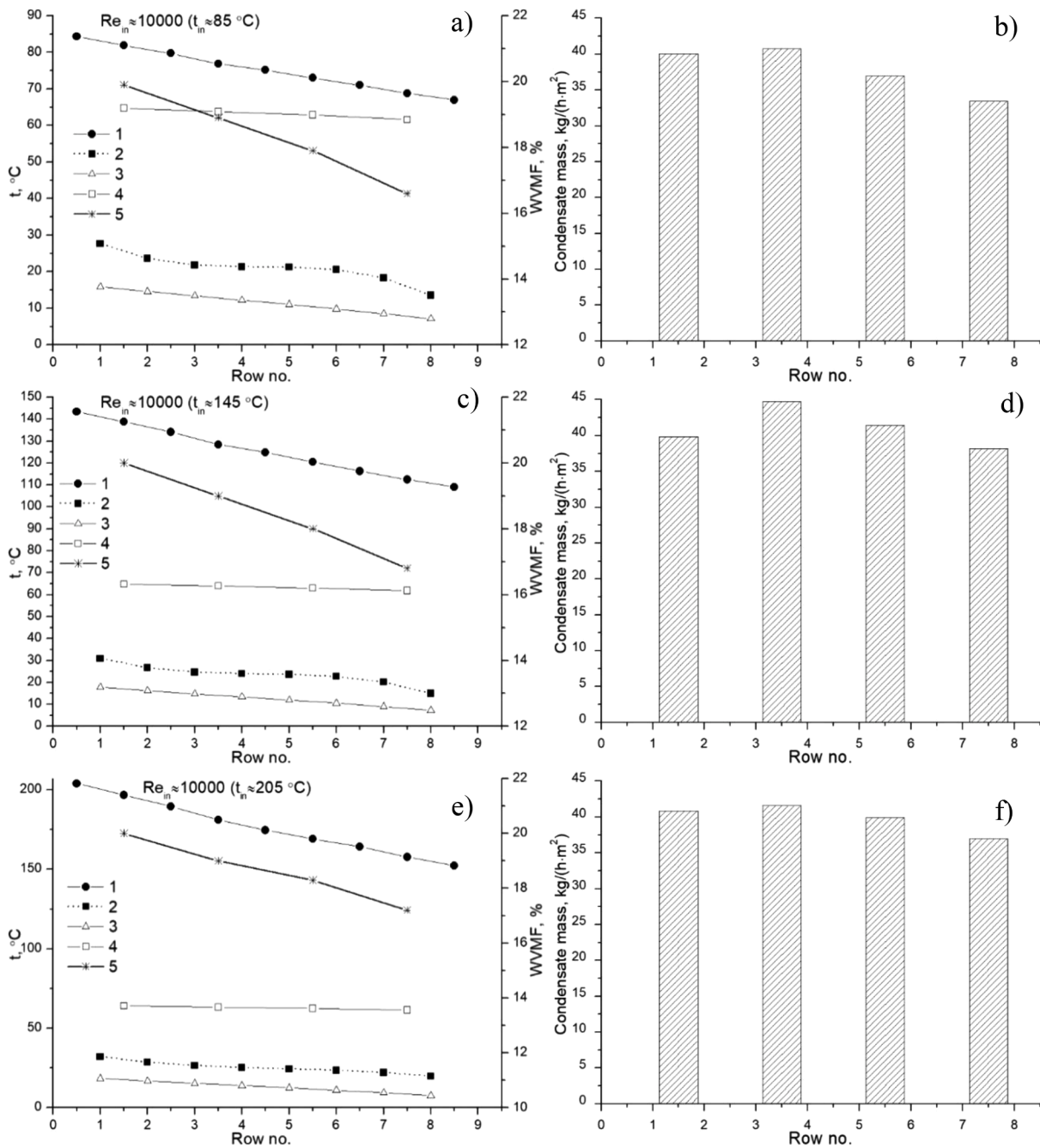
Fig. 12. Temperature, WVMF (a, c, e) and condensate mass variation (b, d, f) along the test section at Re_{in}=10,000, t_{in}=85, 145, 205 °C. (1) average HA temperature, (2) average outside tube wall surface temperature, (3) cooling water temperature, (4) dew point temperature, (5) WVMF. *(2-column fitting image)*.

temperatures, the variation of the condensation in the rows was higher, i.e., about 10–35% from the average value.

3. The average $\overline{Nu}$ numbers in comparison with the dry air $\overline{Nu}$ numbers increased by 1.2–3 times in the case of 10% WVMF and by 1.7–5 times for the WVMF of 20%. The $\overline{Nu}$ numbers decreased with an increase in the humidified air temperature.

4. The condensation efficiency decreased when the Re_{in} was increased from ~35–45% at Re_{in}= 3000 to ~15–25% at Re_{in}=10,000. There is also a significant dependence of the condensation efficiency on the humidified air temperature because, with an increase in this temperature, the condensation efficiency decreased.

5. No clear dependence has been observed of the condensation efficiency on the water vapor mass fraction at the smallest Re_{in} (3000). However, at the highest Re_{in}(10,000), the condensation efficiency for

the WVMF of 20% was higher (~20–25%) than for the WVMF of 10% (~15–20%).

CRediT authorship contribution statement

R. Poškas: Conceptualization, Data curation, Formal analysis, Investigation, Funding acquisition, Methodology, Writing – original draft, Writing – review & editing. **A. Sirvydas:** Conceptualization, Data curation, Formal analysis. **M. Salem:** Conceptualization, Data curation, Formal analysis. **P. Poškas:** Conceptualization, Data curation, Formal analysis, Funding acquisition. **H. Jouhara:** Formal analysis, Funding acquisition, Supervision, Visualization, Writing – original draft.
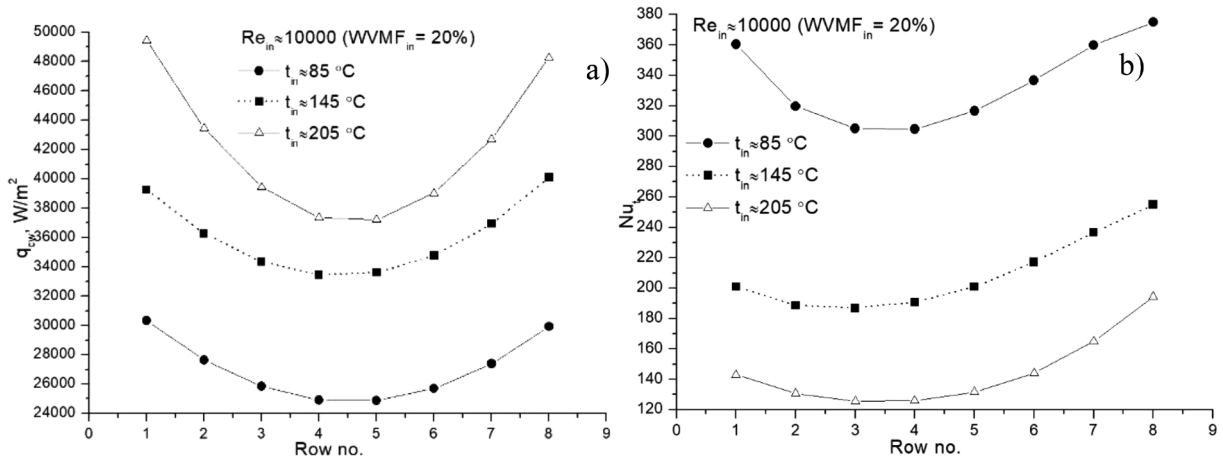
Fig. 13. Heat flux (a) and *Nu* number (b) variationsalong the test section when *Re_{in}*=10,000 at different HA inlet temperatures. *(2-column fitting image)*.
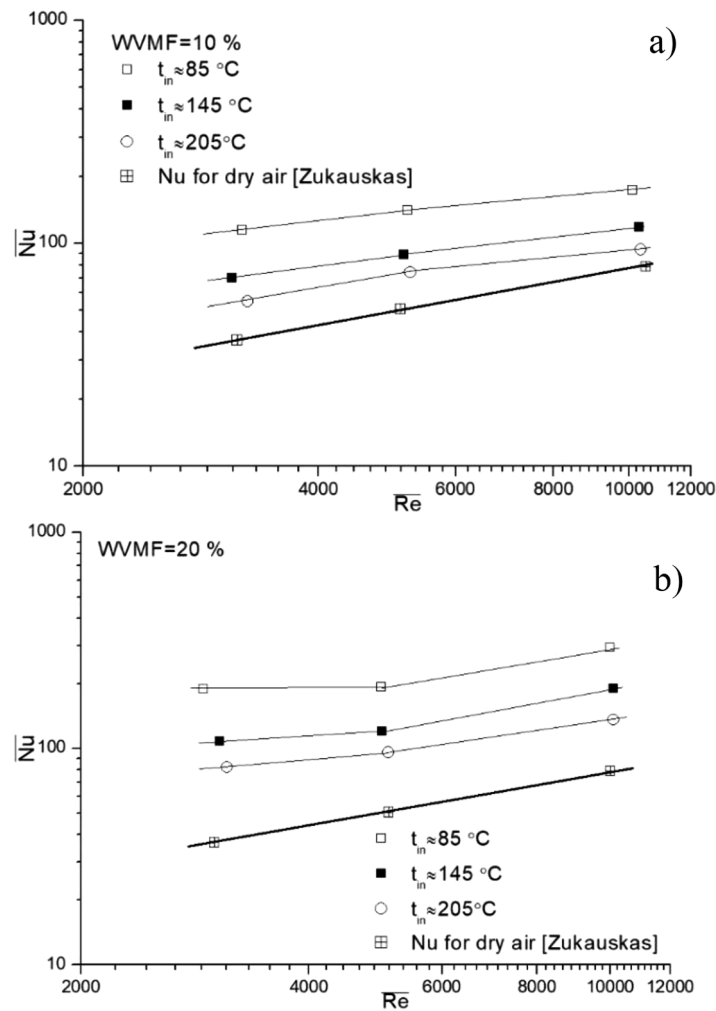

Fig. 14. Comparison of average $\overline{Nu}$ number at different average HA Reynolds numbers and temperatures.*(single column fitting image)*.

Declaration of Competing Interest

The authors declare that they have no known competing financial interests or personal relationships that could have appeared to influence the work reported in this paper.

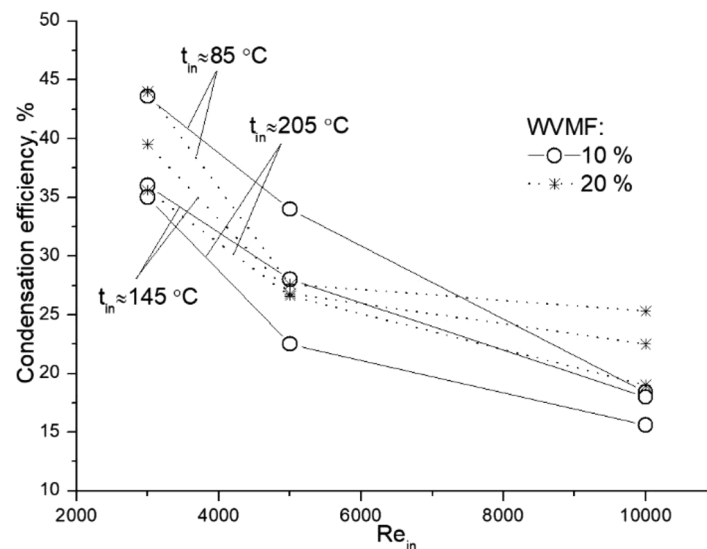### Data availability

Data will be made available on request.

Fig. 15. Comparison of condensation efficiencies at different WVMF, HA inlet Reynolds numbers and temperatures. *(single column fitting image)*.

References

[1] H. Lund, P.A. Østergaard, T.B. Nielsen, S. Werner, J.E. Thorsen, O. Gudmundsson, A. Arabkoohsar, B.V. Mathiesen, Perspectivesonfourthandfifthgenerationdistrictheating, Energy 227 (2021) 120520, https://doi.org/10.1016/j.energy.2021.120520.

[2] P.A. Østergaard, S. Werner, A. Dyrelund, H. Lund, A. Arabkoohsar, P. Sorknæs, O. Gudmundsson, J.E. Thorsen, B.V. Mathiesen, The four generations of district cooling - A categorization of the development in district cooling from origin to future prospect, Energy 253 (2022), 124098, https://doi.org/10.1016/j.energy.2022.124098.

[3] B. El Fil, G. Kini, S. Garimella, A review of dropwise condensation: theory, modelling, experiments, and applications, Int J Heat Mass Transf 160 (2020), 120172, https://doi.org/10.1016/j.ijheatmasstransfer.2020.120172.

[4] M. Jakob, Heat Transfer, Chapter Theory of Film Condensation of Vapor at Rest on Cylindric Surfaces, John Wiley & Sons, 1949, pp. 667–673.

[5] D.Q. Kern, Process Heat Transfer, Chapter Condensation of Single Vapors – Development of Equation for Calculations, McGraw-Hill Book Company, 1950, pp. 263–268.

[6] T. Fujii, H. Uehara, K. Hirata, K. Oda, Heat transfer and flow resistance in condensation of lowpressure steam flowing through tube banks, Int. J. Heat Mass Transf 15 (1972) 247–260, https://doi.org/10.1016/0017-9310(72)90072-5.

[7] J.W. Rose, Effect of pressure gradient in forced convection film condensation on a horizontal tube, Int J Heat Mass Transf 27 (1984) 39–47, https://doi.org/10.1016/0017-9310(84)90235-7.

[8] P.J. Marto, Film condensation heat transfer measurements on horizontal tubes: problems and progress, Experimental Thermal and Fluid Science 5 (1992) 556–569, https://doi.org/10.1016/0894-1777(92)90042-4.

[9] M.W. Browne, P.K. Bansal, An overview of condensation heat transfer on horizontal tube bundles, Appl Therm Eng 19 (1999) 565–594, https://doi.org/10.1016/S1359-4311(98)00055-6.

[10] T. Murase, H.S. Wang, J.W. Rose, Effect of inundation for condensation of steam on smooth and enhanced condenser tubes, Int J Heat Mass Transf 49 (2006) 3180–3189, https://doi.org/10.1016/j.ijheatmasstransfer.2006.02.003.

[11] J.F. Seara, F.J. Uhía, R. Diz, Experimental analysis of ammonia condensation on smooth and integral-fin titanium tubes, International Journal of Refrigeration 32 (2009) 1140–1148, https://doi.org/10.1016/j.ijrefrig.2009.01.026.

[12] C. Bonneaua, C. Josset, V. Melot, B. Auvity, Comprehensive review of pure vapour condensation outside of horizontal smooth tubes, Nuclear Engineering and Design 349 (2019) 92–108, https://doi.org/10.1016/j.nucengdes.2019.04.005.

[13] X. Zhu, S. Chen, S. Shen, Ni S, X. Shi, Q. Qiu, Experimental study on the heat and mass transfer characteristics of air-water two-phase flow in an evaporative condenser with a horizontal elliptical tube bundle, Appl Therm Eng 168 (2020), 114825, https://doi.org/10.1016/j.applthermaleng.2019.114825.

[14] T. Fujii, H. Uehara, Laminar filmwise condensation on a vertical surface, Int J Heat Mass Transf 15 (1972) 217–233, https://doi.org/10.1016/0017-9310(72)90070-7.

[15] T.B. Chang, Mixed-convection film condensation along outside surface of vertical tube in saturated vapor with forced flow, Appl Therm Eng 28 (2008) 547–555, https://doi.org/10.1016/j.applthermaleng.2007.04.012.

[16] P. Kracík, F. Toman, J. Pospíšil, S. Kraml, A Heat Exchanger with Water Vapor Condensation on the External Surface of a Vertical Pipe, Energies 15 (2022) 5636, https://doi.org/10.3390/en15155636.

[17] Y. Liang, D. Che, Y. Kang, Effect of vapour condensation on forced convection heat transfer of moistened gas, Heat and Mass Transfer 43 (2007) 677–686, https://doi.org/10.1007/s00231-006-0148-0.

[18] V. Guichet, H. Jouhara, Condensation, evaporation and boiling of falling films in wickless heat pipes (two-phase closed thermosyphons): a critical review of correlations, Int. J. of Themrofluids 1–2 (2020) 1–37, https://doi.org/10.1016/j.ijft.2019.100001.

[19] V. Guichet, N. Khordehgah, H. Jouhara, Experimental investigation and analytical prediction of a multi-channel flat heat pipe thermal performance, Int. J. of Thermofluids 5–6 (2020) 1–16, https://doi.org/10.1016/j.ijft.2020.100038.

[20] S.J. Meisenburg, R.M. Boarts, W.L. Badger, The influence of small concentrations of air in steam on the steam film coefficient of heat transfer, Trans AIChE 31 (1935) 622–630.

[21] V. Guichet, B. Delpech, H. Jouhara, Experimental investigation, CFD and theoretical modeling of two-phase heat transfer in a three-leg multi-channel heat pipe, Int. J. of Heat and Mass Transfer 203 (2023) 1–27, https://doi.org/10.1016/j.ijheatmasstransfer.2022.123813.

[22] R. Abdullah, J.R. Cooper, A. Briggs, J.W. Rose, Condensation of steam and R113 on a bank of horizontal tubes in the presence of a noncondensing gas, Experimental Thermal and Fluid Science 10 (1995) 298–306, https://doi.org/10.1016/0894-1777(94)00079-N.

[23] M. Osakabe, K. Ishida, K. Yagi, T. Itoh, K. Ohmasa, Condensation Heat Transfer on Tubes in Actual Flue Gas, Heat Transfer - Asian Research 30 (2001) 139–151, https://doi.org/10.1002/1523-1496(200103)30:2<139::AID-HTJ5>3.0.CO;2-0.

[24] M. Osakabe, K. Yagi, T. Itoh, K. Ohmasa, Condensation Heat Transfer on Tubes in Actual Flue Gas (Parametric Study for Condensation Behavior, Heat Transfer - Asian Research 32 (2003) 153–166, https://doi.org/10.1002/htj.10079.

[25] M. Osakabe, N. Ikeda, Condensation Heat Transfer in Wide Range of Non-condensing Gas Fraction, Transactions of the Japan Society of Mechanical Engineers Series B 69 (2003) 2107–2113, https://doi.org/10.1299/kikaib.69.2107.

[26] A. Fouda, M.G. Wasel, A.M. Hamed, E.-S.B. Zeidan, H.F. &Elattar, Investigation of the condensation process of moist air around a horizontal pipe, International Journal of Thermal Sciences 90 (2015) 38–52, https://doi.org/10.1016/j.ijthermalsci.2014.11.022.

[27] H. Li, V. Kottke, Visualization and determination of local heat transfer coefficients in shell-and-tube heat exchangers for staggered tube arrangement by mass transfer measurements, Experimental Thermal and Fluid Science 17 (1998) 210–216, https://doi.org/10.1016/S0894-1777(97)10064-4.

[28] R. Poškas, A. Sirvydas, V. Kulkovas, P. Poškas, An Experimental Investigation of Water Vapor Condensation from Biofuel Flue Gas in a Model of Condenser, (1) Base Case: local Heat Transfer without Water Injection, Processes 9 (5) (2021) 844, https://doi.org/10.3390/pr9050844.

[29] R. Poškas, A. Sirvydas, V. Kulkovas, H. Jouhara, P. Poškas, G. Miliauskas, E. Puida, An Experimental Investigation of Water Vapor Condensation from Biofuel Flue Gas in a Model of Condenser, (2) Local Heat Transfer in a Calorimetric Tube with Water Injection, Processes 9 (8) (2021) 1310, https://doi.org/10.3390/pr9081310.

[30] H.J.H. Brouwers, C.W.M. Geld, Heat transfer, condensation and fog formation in crossflow plastic heat exchangers, Int J Heat Mass Transf 39 (1996) 391–405, https://doi.org/10.1016/0017-9310(95)00113-N.

[31] L. Wang, P. Chen, Y. Zhou, W. Li, C. Tang, Y. Miao, Z. Meng, Experimental study on the condensation of steam with air out of the vertical tube bundles, Frontiers in Energy Research 6 (2018) 1–6, https://doi.org/10.3389/fenrg.2018.00032.

[32] E. Wang, K. Li, N. Husnain, D. Li, J. Maoe, W. Wu, T. Yang, Experimental study on flue gas condensate capture and heat transfer in staggered tube bundle heat exchangers, Appl Therm Eng 141 (2018) 819–827, https://doi.org/10.1016/j.applthermaleng.2018.06.035.

[33] K. Jeong, M.J. Kessen, H. Bilirgen, E.K. Levy, Analytical modeling of water condensation in condensing heat exchanger, Int. J. Heat Mass Transfer 53 (11–12) (2010) 2361–2368, https://doi.org/10.1016/j.ijheatmasstransfer.2010.02.004.

[34] China Electricity Council, China Market Press, Beijing, 2013.

[35] V. Bespalov, L. Beljaev, D. Melnikov, Using Air for Increasing the Depth of the Flue Gas Heat Recovery, in: MATEC web of conferences, 2015.

[36] K. Zhang, Y. Zhang, Z. Wu, Experimental study for radiative heat transfer of high moisture flue gas, J Tsinghua Univ (Sci. Tech) 42 (12) (2002).

[37] Humidity Conversions. Formulas and methods for calculating humidity parameters, Vaisiala (2021).

[38] N.C. Barford, Experimental measurements: Precision, Error and Truth, 2nd ed., John Willey and Sons, New York, 1985.

[39] E.U. Schlunder, K.J. Bell, D. Chisholm, G.F. Hewitt, F.W. Schmidt, D.B. Spalding, J. Tahorek, A. Zukauskas, V. Gnielinski. Heat Exchanger Design Handbook. Begell House Inc., New York, Wallingford (UK) 2003.